RSC Advances

ROYAL SOCIETY OF CHEMISTRY

www.rsc.org/advances

Simultaneous determination of ascorbic acid, dopamine and uric acid at nitrogen-doped carbon nanofiber modified electrode

Jinying Sun[a], Libo Li[b], Xueping Zhang[b], Dong Liu[b], Simin Lv[a], Derong Zhu[a], Tie Wu[a*] and Tianyan You[b*]

[a]School of Pharmacy, Guangdong Medical College, Dongguan 523808, China

[b]State Key Laboratory of Electroanalytical Chemistry, Changchun Institute of Applied Chemistry, Chinese Academy of Sciences, Changchun 130022, China

[a*]Corresponding author, Email: wutie2@163.com (T. Wu), Tel: +86-769-22896547

[b*]Corresponding author, Email: youty@ciac.ac.cn (T. Y. You), Tel: +86-431-85262850

Abstract

The present work described a nitrogen-doped carbon nanofibers modified glassy carbon electrode (NCNF/GCE) for simultaneous detection of ascorbic acid (AA), dopamine (DA) and uric acid (UA). NCNF was prepared by combining electrospinning with thermal treatment method, in which surface etching and nitrogen doping of CNF were achieved by re-utilizing the tail gas produced in thermal treatment procedure. Attributed to the large surface area and N-doped active sites, NCNF exhibited good electrocatalytic performance towards AA, DA and UA. The oxidation potentials were negatively shifted and the current responses were enhanced greatly compared with bare GCE. Large peak to peak potential separations of 277 mV for AA-DA and 124 mV for DA-UA were obtained at NCNF/GCE by differential pulse voltammetry (DPV). Under the optimized conditions, the as-prepared NCNF/GCE exhibited a wider linear range for AA, DA and UA with low detection limits. The proposed method showed high sensitivity, good selectivity and excellent reproducibility and it was successfully applied for real sample analysis.

Introduction

Small biomolecules are related with a variety of biological functions and its concentration levels are regarded as indicators for disease diagnosis.[1] Monitoring small biomolecules such as ascorbic acid (AA), dopamine (DA) and uric acid (UA) in biological fluid is a hot topic in analytical field. AA is not only used for scurvy and cold, but also for mental illness, cancer and AIDS prevention and treatment.[2-4] DA is known as message transfer substance relating with brain functions and human emotions.[5-6] Low levels of DA in cerebral fluids are signs of Parkinson's disease (PD), Alzheimer's disease (AD) and HIV infection.[7-10] On the other hand, uric acid (UA) is the end metabolite of purines and abnormal levels of UA is usually related to gout and hyperuricaemia.[11-14]

Substantial analytical methodologies including high performance liquid chromatography,[15] capillary electrophoresis,[16] UV,[17] chemiluminescence[18] and electrochemical detection[19] have been established for their determination. Electrochemical method is promising for electroactive analytes due to the merits of simplicity, low cost, high sensitivity and good selectivity. Consequently, electrochemical method should be a perspective choice for the determination of AA, DA and UA since they are electroactive compounds. However, AA, DA and UA usually coexist in biological samples and their oxidation potentials are frequently overlapped, thus it is difficult to discriminate and accurately detect them at bare electrode. Therefore, electrode modification is attracting more attentions in practical application.

During the last decades, carbon nanotubes (CNT) and carbon nanofibers (CNF) have shown unique advantages in electroanalysis area due to their fast electron transfer and wide potential window.[20-26] They have common tube-like structures; however, CNF has large amounts of exposed edges at the tip of the circular column, which is expected to possess higher electrocatalytic performance compared with CNT.[27-29] Carbon nanomaterials that doped with hetero atoms such as nitrogen (N) display high electrocatalytic activity towards oxygen reduction reaction (ORR).[30] It is revealed that valence bonds are formed between the introduced nitrogen atoms and neighboring carbon atoms, which can accelerate electron transfer rates.[31-32] N-doped

carbon nanomaterials, including N-doped porous carbon nanopolyhedra, N-doped graphene and N-doped carbon spheres have demonstrated their practical applications in constructing electrochemical sensors.[33-36]

CNF can be prepared by a simple electrospinning combined with thermal treatment procedure in addition to the catalytic thermal chemical vapor deposition growth method.[37-38] However, when N atoms are doped into CNF, a flow of ammonia (NH_3) is usually required for post-treatment, which will make the manipulations more complicated. Herein, surface etching and nitrogen doping were realized with tail gas that generated in the thermal treatment procedure, eliminating the introduction of extra NH_3 flow. The as-prepared NCNF has shown excellent electrocatalytic performance towards O_2 reduction in catalysis area;[39] however, it has not been applied in electroanalysis field. Considering the large surface area and high N-doped active sites in NCNF, it is expected to have good performance towards AA, DA and UA determination.

In the present work, NCNF modified glassy carbon electrode (NCNF/GCE) is served as electrochemical sensor for AA, DA and UA determination by cyclic voltammetry (CV) and differential pulse voltammetry (DPV). The influences of scan rates and buffer pH values are carefully investigated and the electrode reaction kinetics is discussed. Moreover, the peak to peak separation (ΔE_p), linear ranges and limits of detection are also investigated. The results demonstrate that NCNF/GCE has high electrocatatytic activity towards AA, DA and UA and it is suitable for simultaneous determination of AA, DA and UA in practical samples.

Experimental

Reagents and apparatus

All chemicals were of A.R. grade and used directly without further purification. Polyacrylonitrile (PAN, average Mw 150 000), DA, UA and AA (>99%) were purchased from Sigma-Aldrich. Potassium ferricyanide (>99.5%) and dimethylfomamide (DMF, >99.5%) were provided by Beijing Chemical Co., Ltd. Phosphate buffer solution (PBS, 0.1 M) was prepared with 0.1 M Na_2HPO_4 - 0.1 M

NaH_2PO_4 and the pH values were adjusted with 0.1 M H_3PO_4 or 0.1 M NaOH solutions.

The scanning electron microscopy (SEM, PHILIPS XL-30 ESEM) and the transmission electron microscopy (TEM, TECNAI G2) were manipulated with an accelerating voltage of 20 kV and 200 kV, respectively. Three-electrode configuration was used, in which modified or bare GCE was served as working electrode, a Pt rod as counter electrode and an Ag/AgCl (saturated with KCl) as reference electrode (Gauss Union, Wuhan, China). Electrochemical impedance spectroscopy (EIS, Autolab PGSTAT302N) was carried out for the characterization of modified electrodes. Other electrochemical measurements were performed on a CHI 832C electrochemical workstation (CH Instruments, Shanghai, China).

Preparation of NCNF/GCE

NCNF film is prepared according to the procedure described in our previous report.[39] Typically, PAN nanofibers film were obtained by electrospinning a DMF solution containing 10 wt. % PAN, where 18 kV voltage was applied to generate an electric field and the distance between the spinneret and the collector was set at 14 cm. In thermal treatment procedure, an enclosed device was formed using two combustion boats to fully re-utilize the tail gas for the surface etching and doping of N atoms into CNF. The thermal treatment was composed of two steps: (1) stabilization at 300℃ for 60 min, and (2) carbonization at 900℃ for 60 min. All the thermal treatment procedures were performed in nitrogen atmosphere. For the modified electrode, 0.5 mg/mL NCNF was prepared in ethanol by sonication in ultrasonic water bath for about 3 h followed with magnetic stirring for about 2 h. Finally, black and homogeneous NCNF suspensions were obtained. Before modification, bare GCE was polished with 0.05 μm alumina in water slurry on a polishing cloth and rinsed with water, ethanol and water successively. And then, 6 μL of the resultant NCNF suspensions were dropped on GC substrate. For comparison, CNF/GCE was also prepared with the same procedure to NCNF/GCE. The newly prepared modified electrodes were left in air to dry for further use.

Electrochemical measurement

CV (within a potential range of -0.2 V - +0.8 V) and EIS (within a frequency range of 0.01 - 10^5 Hz) for characterization of the modified electrodes were carried out in 5 mM $K_3Fe(CN)_6/K_3Fe(CN)_6$ (containing 0.1 M KCl) and other electrochemical tests were performed in 0.1 M PBS (pH 4.5). DPV was carried out in the potential range of -0.2 V to +0.8 V and it was used for AA, DA and UA determination. In order to rule out the possible contamination from counter electrode,[40] the electrolyte and reaction solution were often replaced, and the working electrode was often rinsed with buffer solution.

Sample preparation

Stock solutions of 10 mM AA, DA and UA were prepared in deionized water and stored at 4℃. Lower concentrations of AA, DA and UA were obtained by diluting stock solutions with 0.1 M PBS and newly prepared every day.

DA hydrochloride injection solution (purchasing from local hospital) was firstly diluted by 10-fold with deionized water and then diluted by 1000-fold with 0.1 M PBS (pH 4.5). Concentrated standard solutions of DA were added into the diluted DA injections.

Human urine was collected from a healthy female and filtered with a 0.22 μm membrane before any other manipulations. Filtered urine was diluted with 0.1 M PBS (pH 4.5) by 350-fold with 0.1 M PBS (pH 4.5). In recovery rate experiments, concentrated standard solutions of UA were added into the diluted urine samples.

Results and discussions

Characterization of NCNF and modified electrodes

Surface morphology of CNF and NCNF and their structures were characterized by SEM and TEM. Compared with CNF (Fig. 1A), the prepared NCNF (Fig. 1B) exhibited a smaller diameter of 143 ± 20 nm in average than CNF (259 ± 22 nm), which would be attributed to the incorporation of N atoms. Moreover, a rougher surface with more defects of NCNF (Fig. 1D) was observed than CNF (Fig. 1C). The small diameter and rougher surface would accelerate the electron transfer rate between the analytes and the electrode. Therefore, NCNF/GCE was expected to have

a large surface area and fast electron transfer ability due to the rough surface and defects which formed by surface etching with tail gas.

The electrochemical properties of the prepared NCNF/GCE was characterized by CV and EIS using $K_3Fe(CN)_6/K_4Fe(CN)_6$ as redox probe. At the bare GCE, ΔE_p for the redox peaks was 128 mV. When modified with CNF, the ΔE_p was reduced to 105 mV. At NCNF/GCE, the ΔE_p was further reduced to 93 mV (Fig. 2A). The results showed that CNF was beneficial for electron transfer and the introduction of N atoms into CNF could further accelerate the electron transfer rate. The anodic peak current was 19.49 μA at bare GCE, and increased to 25.57 μA and 43.96 μA at CNF/GCE and NCNF/GCE, respectively. Electroactive surface area (A) could be calculated according to the following formula: $I_p = 2.69\times10^5 AD^{1/2}n^{3/2}\gamma^{1/2}C$, where D is the diffusion coefficient (6.7×10^{-6} cm^2/s); C is the concentration of redox probe (5×10^{-6} mol/cm^3); n is the electron transfer number (n = 1) and γ is the san rate (0.05 V/s). According to the formula, the electroactive surface areas were calculated to be 0.025 cm^2, 0.033 cm^2 and 0.056 cm^2 for GC, CNF/GCE and NCNF/GCE, respectively. Therefore, the electroactive surface area of the bare GCE was slightly magnified with CNF modification and further magnified with NCNF modification. EIS was powerful in investigating the electrochemical kinetics occurred at the interface of electrode/electrolyte, therefore it was used for the characterization of NCNF/GCE. The circular part in the Nyquist diagram reflects the electron transfer process. Larger diameter in the circular curve represents higher electron transfer resistance (R_{ct}) at the interface of electrode/electrolyte. As depicted in Fig.2B, a well-defined semicircle was observed for bare GCE with a high R_{ct} of 1.33 kΩ. As for CNF/GCE and NCNF/GCE (Inset of Fig. 2B), only a small semicircle appeared, indicating that the R_{ct} was greatly decreased. The results were in accordance with CV results, suggesting that the conductivity and the electron transfer rate were well improved at NCNF modified electrode.

Electrochemical behaviors of AA, DA and UA

Based on the good conductivity, high electron transfer rate and large electroactive surface area, NCNF was employed to investigate the electrochemical behavior of AA,

DA and UA using CVs (Fig. 3). The oxidation of 1 mM AA at different electrodes was shown in Fig. 3A. As depicted, a broad oxidation peak of AA at 0.408 V was observed at bare GCE. No corresponding reduction peak was observed, indicating that the oxidation of AA at bare GCE was an irreversible procedure. At CNF/GCE, the oxidation peak of AA negatively shifted to 0.325 V. However, it was still a broad oxidation peak. Interestingly, at NCNF/GCE, a sharp anodic peak of AA was obtained, accompanied with the oxidation potential negatively shifted to 0.139 V. The slow electron transfer rate of AA at bare GCE and CNF/GCE perhaps resulted from the electrode fouling by the oxidation product of AA. In contrast, N-doped active sites greatly improved the roughness of surface and electroactive area, both of which accelerated the electron transfer rates.

Different from the electrochemical behavior of AA, DA exhibited a well-defined redox couple at NCNF/GCE, indicating the good reversibility of DA (Fig. 3B). However, compared with CNF/GC electrode, although the ΔE_p decreased from 122 mV to 85 mV at NCNF/GCE, the oxidation potentials of DA only changed a little, which was different with AA. In addition, the oxidation current of DA at NCNF/GCE was 3.87-fold higher than bare GCE and 1.64-fold higher than CNF/GCE. The improved reaction reversibility and enhanced peak current suggested that NCNF/GCE had an excellent electrocatalytic activity towards DA.

As for UA (Fig. 3C), it can be seen that the oxidation of UA at bare GCE and CNF/GCE were absolutely irreversible. In contrast, a corresponding cathodic peak appeared at NCNF/GCE, indicating that the reversibility was greatly improved.

To further validate the applicability of NCNF/GCE, CV behavior was investigated for ternary mixture of AA, DA and UA (Fig. 3D). At the bare GCE, the oxidation peaks were overlapped completely. When modified with CNF, the oxidation current response was a bit increased. However, it was still difficult to detect AA, DA and UA simultaneously because the oxidation peaks could not be separated completely. Distinctively, three sharp and well defined peaks could be observed at 0.198 V, 0.476 V and 0.611 V corresponding to AA, DA and UA, respectively at NCNF/GCE. Large ΔE_p was obtained for AA-DA (278 mV) and DA-UA (141 mV), respectively. On the

other hand, current responses of AA, DA and UA were enhanced at NCNF/GCE. Consequently, it was practical to detect AA, DA and UA at NCNF/GCE.

Effect of scan rate

To acquire the kinetics of electrode reactions, cyclic voltammograms at different scan rates for AA, DA and UA were investigated. CVs of AA oxidation with different scan rates (15-40 mV/s) at NCNF/GCE were shown in Fig. 4A. The oxidation currents (I_{pa}) were linear with square root of scan rate ($v^{1/2}$) (inset plot) and the regression equation could be expressed as (1):

$$I_{pa}(\mu A) = 0.3898\text{-}0.5122v^{1/2}\,(mV/s)\ (r^2=0.999) \quad (1)$$

A well redox couple appeared for DA electrochemical oxidation (Fig. 4B). Both the anodic currents and cathodic currents plotted with square root of scan rates (50-500 mV/s) displayed good linear relationships, which could be expressed as (2) and (3):

$$I_{pa}(\mu A) = 3.6858\text{-}0.8962v^{1/2}(mV/s)\ (r^2=0.995) \quad (2)$$

$$I_{pc}(\mu A) = -5.2742+1.112v^{1/2}(mV/s)\ (r^2=0.998) \quad (3)$$

The cathodic current response was nearly equal to the corresponding anodic current response, revealing that DA exhibited good reversibility at NCNF/GCE.

As for UA, the oxidation currents increased with the higher scan rates (10-500 mV/s) (Fig. 4C). I_{pa} was linear with the square root of scan rates as following regression equation (4):

$$I_{pa}(\mu A) = 0.4686\text{-}0.6439v^{1/2}(mV/s)\ (r^2=0.997) \quad (4)$$

The results showed that for AA, DA and UA, the process was diffusion-controlled at NCNF/GCE.

Effect of buffer pH value

Since protons were reported to participate in the electrode reactions of AA, DA and UA, the influence of buffer pH were carefully investigated in the pH range of 3.5-7.0 with 0.5 pH interval. As shown in Fig. 5, oxidation potentials of all the analytes negatively shifted with the increase of pH value, indicating that all the procedures were pH-dependent reactions. Furthermore, there were excellent linear relationships between oxidation potentials and buffer pH values, which could be expressed as

follows:

$$E_{pa}\,(V) = 0.292\text{-}0.044pH\ (r^2=0.982) \quad (AA)$$

$$E_{pa}\,(V) = 0.606\text{-}0.059pH\ (r^2=0.992) \quad (DA)$$

$$E_{pa}\,(V) = 0.713\text{-}0.058pH\ (r^2=0.989) \quad (UA)$$

The slopes of 44 mV/pH for AA, 59 mV/pH for DA and 58 mV/pH for UA were close to the theoretical value of 59 mV/pH in Nernst equation at 25℃, meaning that all the compounds underwent equal electron and equal proton electrocatalytic oxidation processes at NCNF/GCE. At the same time, buffer pH value also influences the oxidation currents of three analytes (data not shown here). In addition, acidic buffer was more beneficial for obtaining sharp and high current response using NCNF/GCE. As buffer pH increased higher than pH 5.5, the oxidation current responses of all the three analytes sharply decreased. Therefore, 0.1 M PBS of pH 4.5 was chosen for highly sensitive and selective detection and simplifying the experiment procedure.

Simultaneous determination of AA, DA and UA

Fig. 6 showed the electrochemical responses of ternary mixture containing 1 mM AA, 50 μM DA and 50 μM UA at bare GCE and modified electrodes. Similar with the results in Fig. 5, only two broad and coterminous oxidation peaks appeared at the bare GCE, indicating that simultaneously detect AA, DA and UA was impossible. After the modification with CNF at GC electrode, three oxidation peaks close to each other were observed. However, ΔE_p of AA-DA and DA-UA was so small that they still could not be well discriminated in ternary mixtures. In contrast, three well-defined and sharper oxidation peaks corresponding to AA (0.109 V), DA (0.386 V) and UA (0.510 V) were observed at NCNF modified electrode. The distinctive and improved electrocatalytic properties of NCNF/GCE were perhaps attributed to the N-doped active sites and large electroactive area.

When electrochemical measurements were performed for linear ranges investigation, two other components concentrations were kept constant and only the target component concentration varied. Excellent linear relationships between the current responses and analytes concentrations were obtained for AA, DA and UA

(Table1).

Table1 Analytical parameter for simultaneous determination of AA, DA and UA at NCNF/GCE.

Compounds	Linear range (μM)	Linear equation	R^2	LOD (μM)
AA	50 ~ 3000	$I_{pa} = 0.465 + 0.005C$	0.998	50
DA	1 ~ 10	$I_{pa} = -0.194 + 0.346C$	0.998	0.5
	10 ~ 200	$I_{pa} = 2.678 + 0.115C$	0.992	
UA	5 ~ 200	$I_{pa} = 1.681 + 0.053C$	0.992	1

Ternary mixtures of 500 μM AA, 50 μM DA and 100 μM UA was used for the reproducibility examination. RSDs of AA, DA and UA at the same NCNF modified electrode were13.8%, 1.93% and 1.79%, respectively (n=10).

Table 2 Comparison of NCNF/GCE with other modified electrodes for the determination of AA, DA and UA.

Modified electrodes	Linear ranges (AA, DA, UA)	LOD (AA, DA, UA)	AA-DA (mV)	DA-UA (mV)
$NanoSnO_2$/MWCNT modified CPE[41]	100-5000 μM 0.3-50 μM 3-200 μM	50 μM 0.03 μM 1 μM	150	17
DWCNT/choline modified GCE[42]	0.1-777 μM 0.06-314 μM 0.25-344 μM	0.03 μM 0.03 μM 0.05 μM	182	146
SWCNT modified GCE[43]	15-800 μM 0.5-100 μM 0.55-90 μM	6.68 μM 0.28 μM 0.26 μM	260	145
nitrogen-doped carbon hollow spheres[33]	1-400 μM (DA) 5-350 μM (UA)	0.3 μM (DA) 1 μM (UA)	N	N
nitrogen-doped porous carbon nanopolyhedra modified GCE[34]	80-2000 μM 0.5-30 μM 4-50 μM	740 nM 11 nM 21 nM	228	124
hollow nitrogen-doped carbon spheres-reduced graphene oxide modified GCE[36]	50-1200 μM 0.5-90 μM 1-70 μM	650 nM 12 nM 18 nM	252	132
NCNF/GCE (this work)	50-3000 μM 1-10 μM, 10-200 μM 5-200 μM	50 μM 0.5 μM 1 μM	277	124

Note: "N" represents that it was not mentioned

The analytical performance of NCNF/GCE was compared with carbon nanotubes and other nitrogen-doped carbon materials (Table 2). It can be seen that at NCNF/GCE, the peak to peak potential separation of AA-DA (277 mV) was higher than any other materials, and the ΔE_p of DA-UA was comparable with others.[41-43]

Linear ranges for AA, DA and UA obtained at NCNF/GCE was wider than at nitrogen-doped porous carbon nanopolyhedra modified GCE[34] and hollow nitrogen-doped carbon spheres-reduced graphene oxide modified GCE.[36] The results showed that AA, DA and UA could be simultaneously determined at NCNF/GCE with high sensitivity and excellent selectivity. The enhanced sensing performance after nitrogen doping may be attributed to the generation of more structural defects and edge plane by etching the surface of CNF. Importantly, the higher content of pyrrolic-N at the edges of graphene layers would contribute to the improved performance because this type of N atoms possesses higher charge mobility and better donor-acceptor properties.[39]

Applications

The proposed method was utilized to investigate the real samples. Recoveries of DA and UA in DA hydrochloride drug injection and human urine respectively were measured by standard addition method. As shown in Table 3, the recoveries were between 91.1% and 96.0% and RSDs were between 0.8% and 5.2% (n = 3) respectively, indicating that the determination for real samples was of high accuracy at the constructed sensor. High accuracy and good reproducibility for real samples at NCNF/GCE showed that it was qualified for practical applications.

Table 3 Practical applications of the proposed method (n = 3).

samples	Specific（μM）	Added （μM）	Found （μM）	Recovery（%）	RSD （%） (n = 3)
DA injection	5	0	4.80	96.0	2.3
		10	14.0	93.3	0.8
		40	41.0	91.1	1.4
Urine sample	9.8	0	9.8	-	0.9
		10	18.9	95.9	5.2
		30	37.4	94.1	4.8

Conclusions

In this work, a nitrogen-doped carbon nanofiber film was prepared with a simple electrospinning combined with thermal treatment. NCNF/GCE exhibited high electrocatalytic activity towards the oxidation of AA, DA and UA due to the N-doped active sites, large electroactive area and high specific surface area. The preparation of NCNF film and NCNF/GCE is simple and easy to be reproduced, thus it is promising for AA, DA and UA determination in biological samples.

Acknowledgements

This work was supported by Innovation Fund of Guangdong Medical College (STIF201112) and Postdoctoral Research Foundation from Guangdong Medical College (XB1123).

References

1 C. J. Feng, S. Dai and L. Wang, *Biosens. Bioelectron.*, 2014, **59**, 64.

2 L. Zhang, W. J. Yuan and B. Q. Hou, *J. Elechroana. Chem.*, 2013, **689**, 135.

3 J. Du, R. R. Yue, F. F. Ren, Z. Q. Yao, F. X. Jiang, P. Yang and Y. K. Du, *Biosens. Bioelectron.*, 2014, **53**, 220.

4 X. F. Liu, L. Zhang, S. P. Wei, S. H. Chen, X. Ou and Q. Y. Lu, *Biosens. Bioelectron.*, 2014, **57**, 232.

5 W. Zhang, Y. Q. Chai, R. Yuan, S. H. Chen, J. Han and D. H. Yuan, *Anal. Chim. Acta*, 2012, **756**, 7.

6 K. R. Mahanthesha and B. E. K. Swamy, *J. Electroanal. Chem.*, 2013, **703**, 1.

7 M. Roushani, M. Shamsipur and H. R. Rajabi, *J. Elechroanal. Chem.*, 2014, **712**, 19.

8 C. F. Wang, P. P. Xu and K. L. Zhuo, *Electroanalysis*, 2014, **26**, 191.

9 S. J. Yu, C. H. Luo, L. W. Wang, H. Peng and Z. Q. Zhu, *Analyst*, 2013, **138**, 1149.

10 Z. Temocin, *Sensor Actuat. B: Chem.*, 2013, **176**, 796.

11 T. Q. Xu, Q. L. Zhang, J. N. Zheng, Z. Y. Lv, J. Wei, A. J. Wang and J. J. Feng,

Electrochim. Acta, 2014, **115**, 109.

12 S. P. Kumar, R. Manjunatha, T. V. Venkatesha and G. S. Suresh, *Russion J. Electrochem*., 2013, **49**, 339.

13 Y. Y. Yu, Z. G. Chen, B. B. Zhang, X. C. Li and J. B. Pan, *Talanta*, 2013, **112**, 31.

14 D. Wu, Y. Y. Li, Y. Zhang, P. P. Wang, Q. Wei and B. Du, *Electrochim. Acta*, 2014, **116**, 244.

15 K.E. Hubbard, A. Wells, T.S. Owens, M. Tagen, C.H. Fraga and C.F. Stewart, *Biomed.Chromotogr*.,2010, **24**, 626.

16 X. L. Wang, L. J. Li, Z. Y. Li, J. Wang, H. Y. Fu and Z. Z. Chen, *J. Electroanal. Chem*., 2014, **712**, 139.

17 L. Fraisse, M.C. Bonnet, J.P. De Farcy, C. Agut, D. Dersigny and A. Bayol, *Anal.Biochem*., 2002,**309**,173.

18 H. Chen, R.B. Li, L. Lin, G.S. Guo, J.M. Lin, *Talanta*,2010,**81**,1688.

19 H. X. Li, Y. Wang, D. X. Ye, J. Luo, B. Q.Su, S. Zhong and J. L. Kong, *Talanta*, 2014, **127**, 255.

20 Y. H. Wang, X. X. He, K. M. Wang, J. Su, Z. F. Chen, G. P. Yan and Y. D. Du, *Biosens. Bioelectron.*, 2013, **41**, 238.

21 G. Z. Liu, W. Q. Guo and D. D. Song, *Biosens. Bioelectron.*, 2014, **52**, 360.

22 R. Akter, M. A. Rahman and C. K. Rhee, *Anal. Chem*., 2012, **84**, 6407.

23 J. E. Koehne, M. Marsh, A. Boakye, B. Douglas, I. Y. Kim, S. Y. Chang, D. P. Jang, K. E. Bennet, C. Kimble, R. Andrews, M. Meyyappan and K. H. Lee, *Analyst*, 2011, **136**, 1802.

24 L. C. Feng, N. Xie and J. Zhang, *Materials*, 2014, **7**, 3919.

25 Y. Liu, J. S. Huang, D. W. Wang, H. Q. Hou and T. Y. You, *Anal. Methods*, 2010, **2**, 855.

26 Y. F. Li, L. Syed, J. W. Liu, D. H. Hua and J. Li, *Anal. Chim. Acta*, 2012, **744**, 45.

27 V. Vamvakaki, M. Hatzimarinaki and N. Chaniotakis, *Anal. Chem*., 2008, **80**, 5970.

28 J. S. Huang, Y. Liu and T. Y. You, *Anal. Methods*, 2010, **2**, 202.

29 P. Serp, M. Corrias and P. Kalck, *Appl. Catalysis A: Gneneral*, 2003, **253**, 337.

30 C. H. Choi, S. H. Park and S. I. Woo, *ACS Nano*, 2012, **6**, 7084.

31 S. U. Lee, R. V. Belosludov, H. Mizuseki and Y. Kawazoe, *Small*, 2009, **5**, 1769.

32 K. P. Gong, F. Du, Z. H. Xia, H. Z. Xia, M. Durstock and L. M. Dai, *Science*, 2009, **323**, 760.

33 Y. Li, M. Yao, T. T. Li, Y. Y. Song, Y. J. Zhang and S. Q. Liu, *Anal. Methods*, 2013, **5**, 3635.

34 P. B. Gai, H. J. Zhang, Y. S. Zhang, W. Liu, G. B. Zhu and X. H. Zhang, *J. Mater. Chem. B*, 2013, **1**, 2742.

35 S. M. Li, S. Y. Yang, Y. S. Wang, C. H. Lien, H. W. Tien, S. T. Hsiao, W. H. Liao, H. P. Tsai, C. L. Chang, C. C. M. Ma, C. C. Hu, *Carbon*, 2013, **59**, 418.

36 H. J. Zhang, P. B. Gai, R. Cheng, L. Wu, X. H. Zhang and J. H. Chen, *Anal. Methods*, 2013, **5**, 3591.

37 S. Ko, T. Tatsuma, A. Sakoda, Y. Sakai and K. Komori, *Phys. Chem. Chem. Phys.*, 2014, **16**, 12209.

38 J. G. Lawrence, L. M. Berhan and A. Nadarajah, *ACS Nano*, 2008, **6**, 1230.

39 D. Liu, X. P. Zhang, Z. C. Sun and T. Y. You, *Nanoscale*, 2013, **5**, 9528.

40 C. K. Gu, B. C. Norris, F. F. Fan, C. W. Bielawski,A. J. Bard, *ACS Catal.,* 2012, **2**, 746.

41 D. M. Sun, Q. Zhao, F. Tan, X. C. Wang and J. S. Gao, *Anal. Methods*, 2012, **4**, 3283.

42 B. B. Xu, Q. J. Song and H. H. Wang, *Anal. Method*, 2014, **5**, 2335.

43 J. Balamurugan, S. M. S. Kumar, R. Thangamuthu and A. Pandurangan, *J. Mol. Catala.: Chem*., 2013, **372**, 13.

Captions

Fig.1 SEM (A and B) and TEM (C and D) of CNF (A and C) and NCNF film (B and D).

Fig.2 CV (A) and EIS (B) at bare GCE (a), CNF/GCE (b) and NCNF/GCE (c) in 5 mM $Fe(CN)_6^{3-/4-}$ (0.1 M KCl).

Fig.3 CVs responses of 1mM AA (A), 0.2 mM DA (B),0.5 mM UA (C) and their ternary mixtures (D) at bare GCE (a); CNF/GCE (b) and NCNF/GCE (c) in 0.1 M PBS (pH 4.5). Conditions: potential range, -0.2 V to +0.8 V; scan rate, 50 mV/s.

Fig.4 CVs of 0.5 mM AA (A), 0.1 mM DA (B) and 0.2 mM UA (C) at different scan rates at NCNF/GCE in 0.1 M PBS (pH 4.5); Insets were the plots of the oxidation currents with square root of scan rates

Fig.5 Effect of buffer pH on oxidation potential of ternary mixiture of 1 mM AA, 50 μM DA and 50 μM UA at NCNF/GCE by DPV in 0.1 M PBS. Conditions: pulse interval, 200 ms; pulse amplitude, 50 mV; pulse width: 50 ms.

Fig.6 DPV of 1 mM AA, 50 μM DA and 50 μM UA at bare GCE (a), CNF/GCE (b) and NCNF/GCE (c) in 0.1 M PBS (pH 4.5). Conditions were the same as in Fig.5.

TOC This paper demonstrates high electrocatalytic activity of NCNF/GCE towards small biomolecules. The proposed electrochemical sensor exhibits good selectivity, high sensitivity and excellent stability towards AA, DA and UA simultaneous detection.

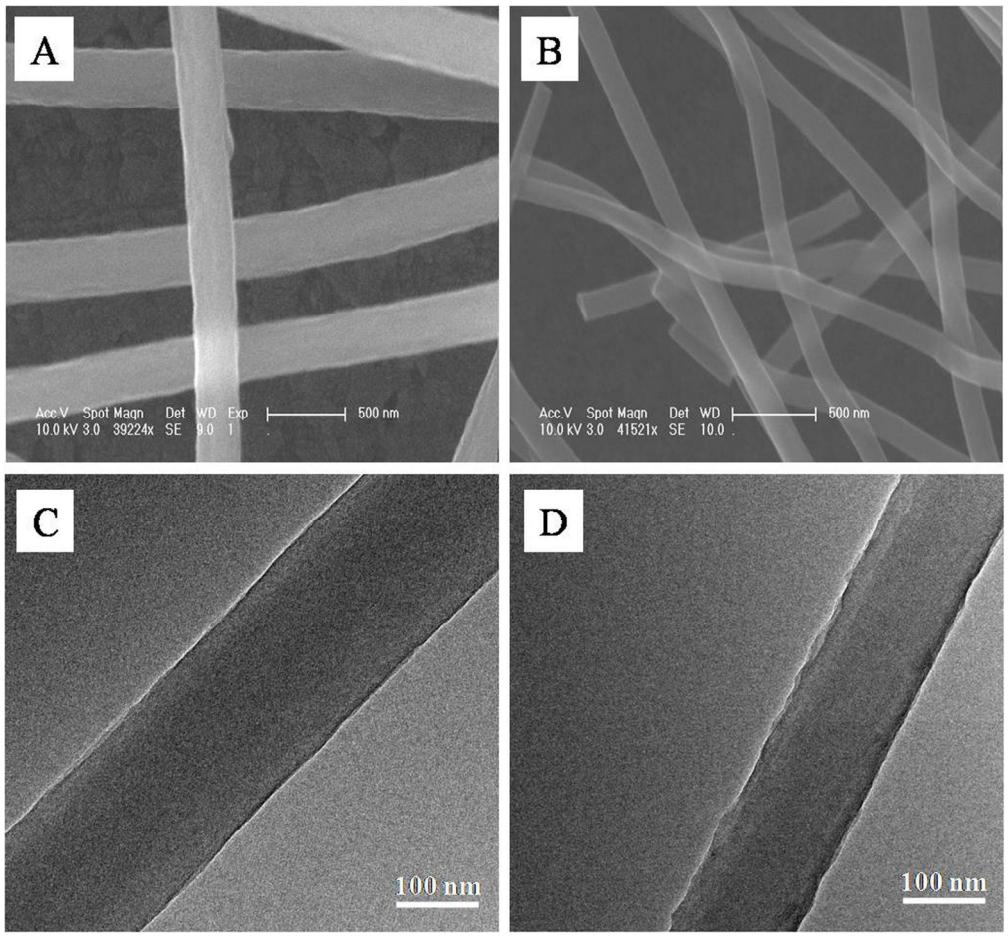

162x150mm (300 x 300 DPI)

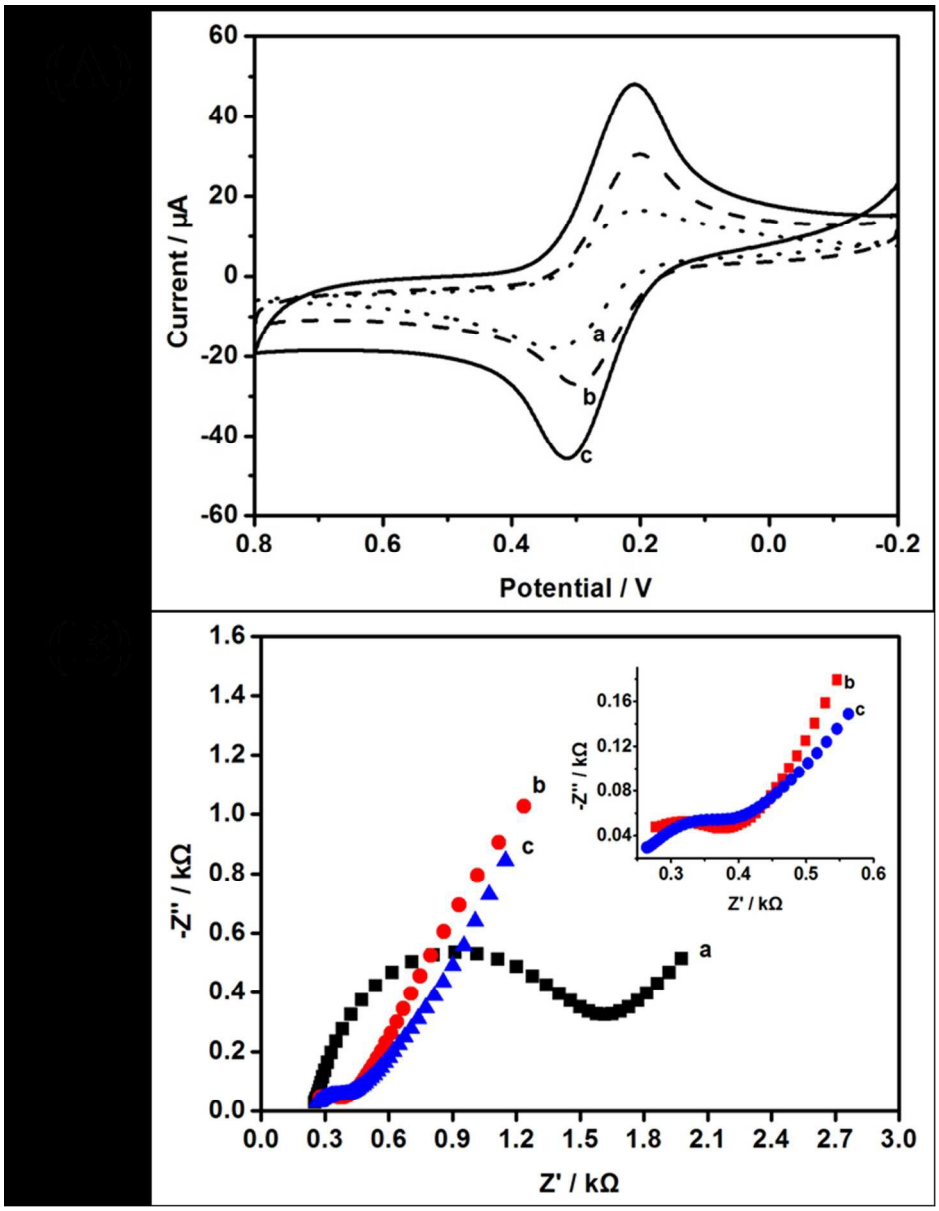

160x206mm (300 x 300 DPI)

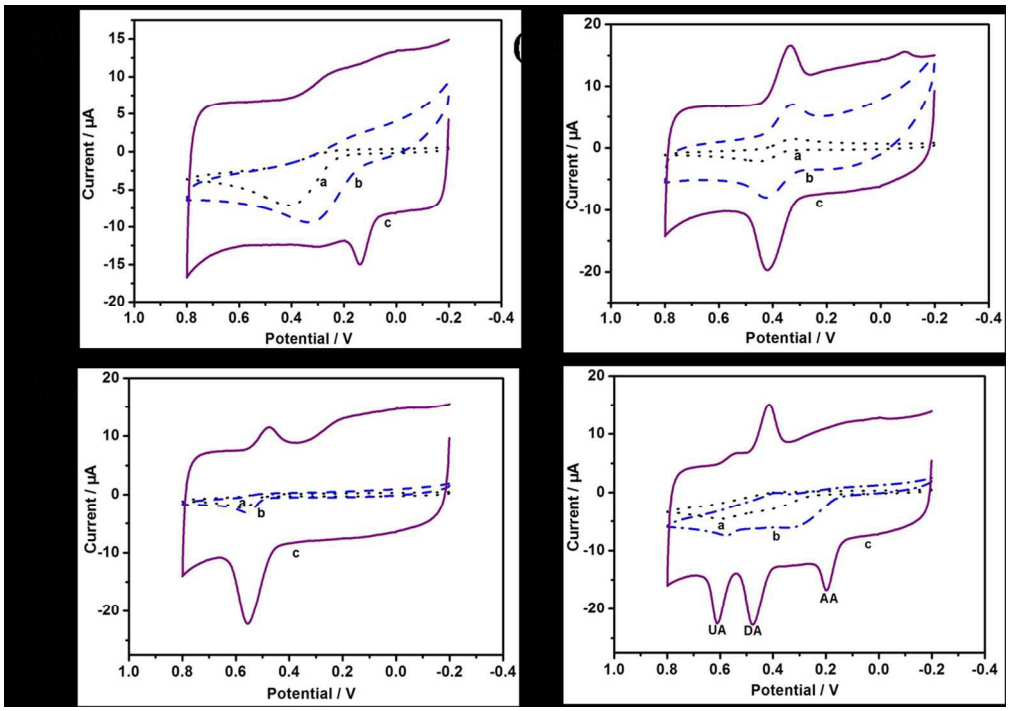

165x116mm (300 x 300 DPI)

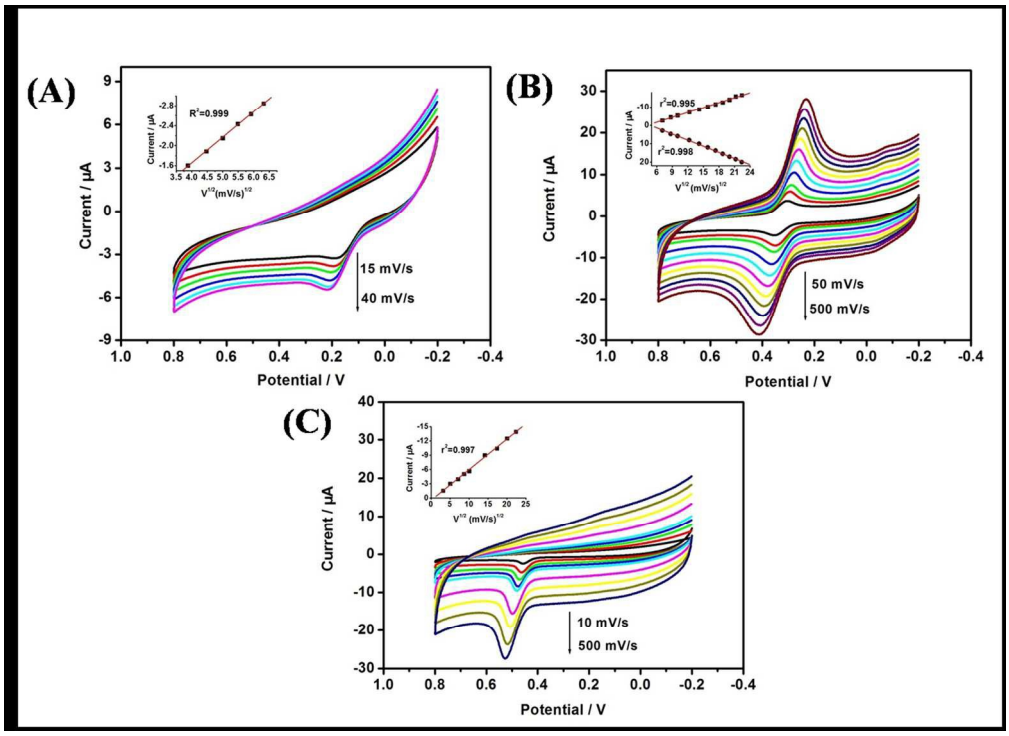

173x125mm (300 x 300 DPI)

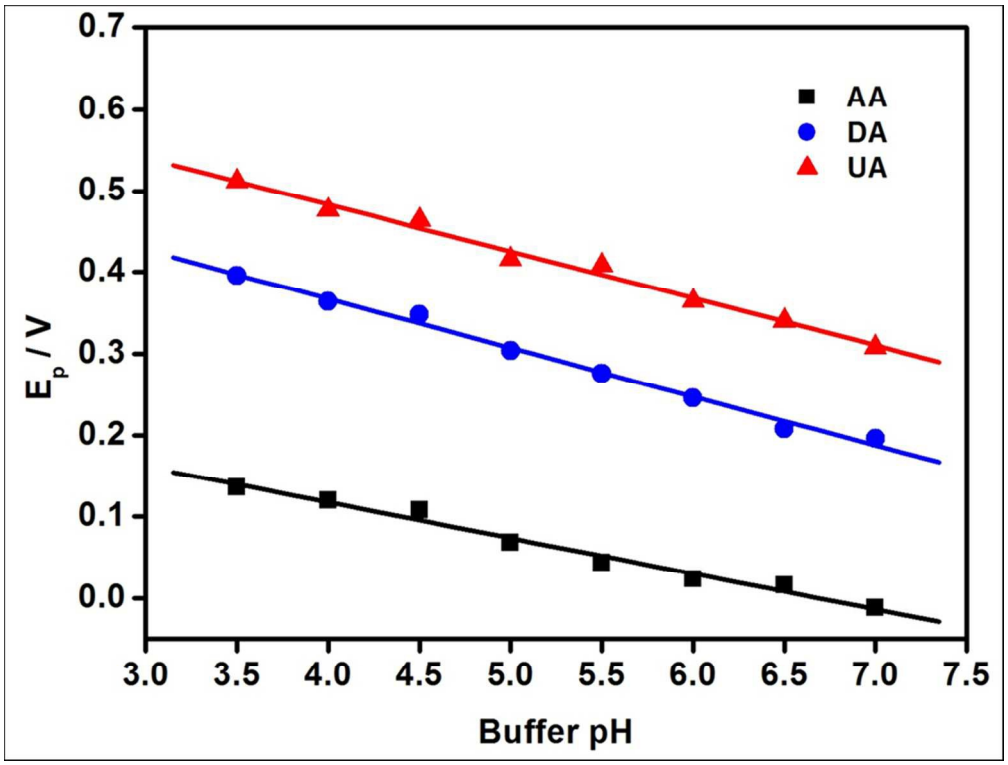

120x90mm (300 x 300 DPI)

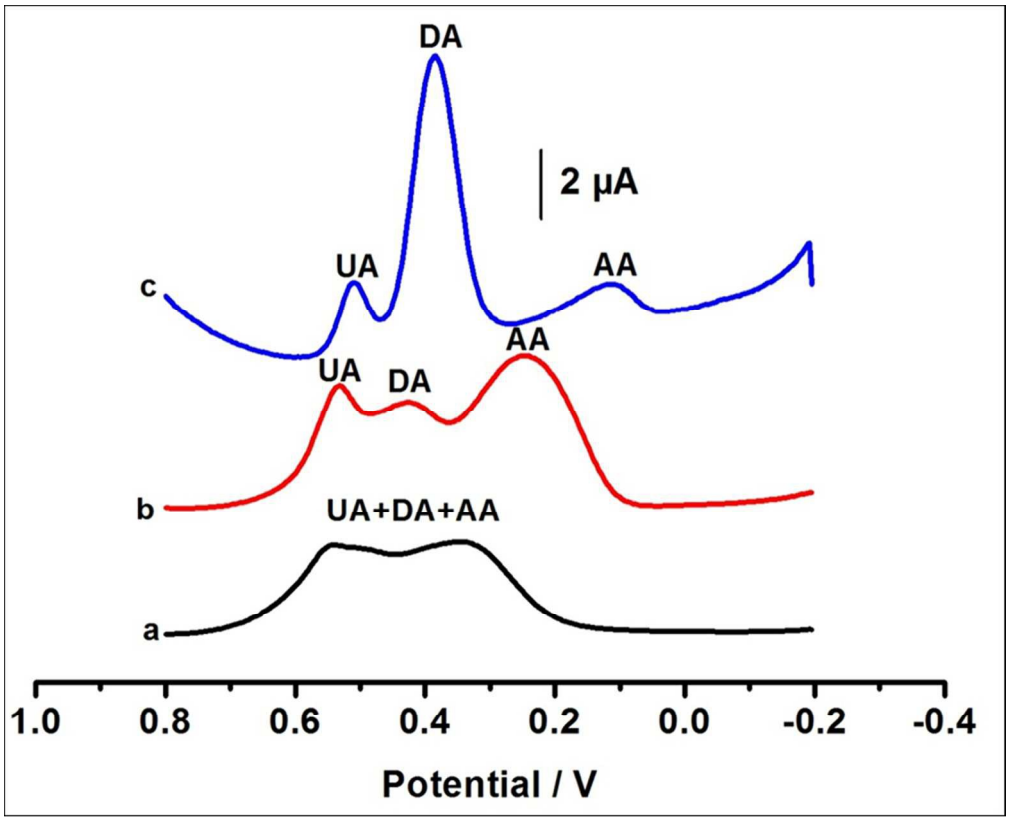

120x97mm (300 x 300 DPI)

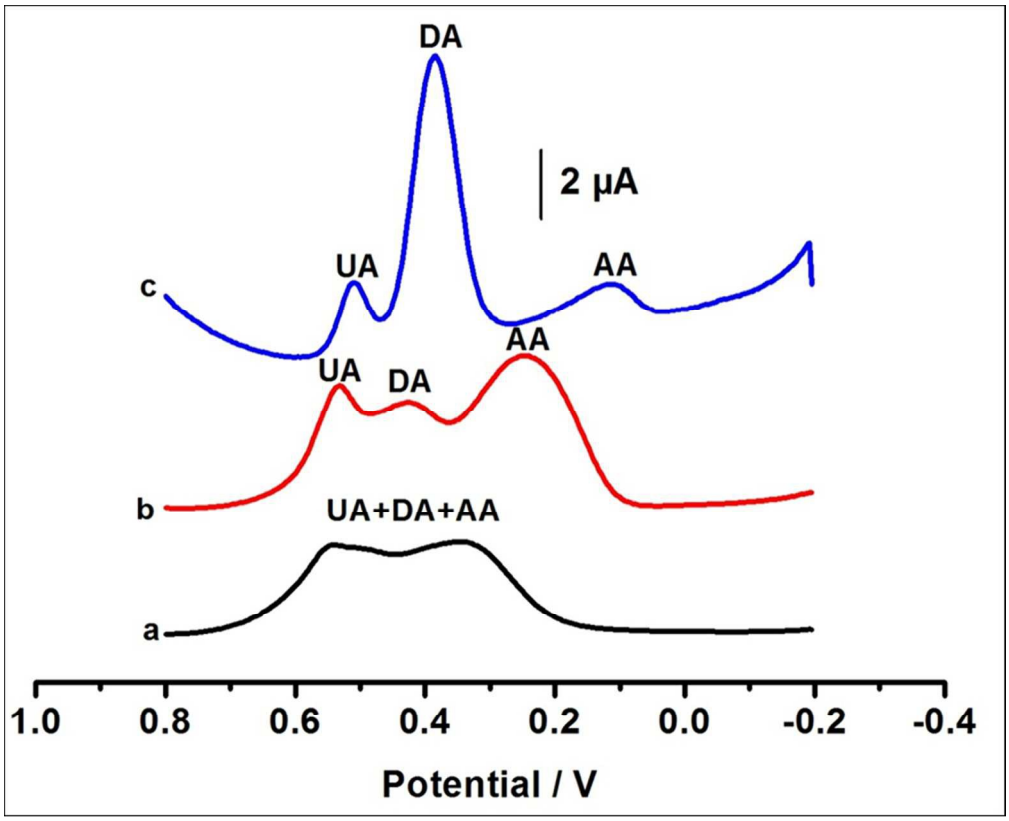

120x97mm (300 x 300 DPI)